ORIGINAL RESEARCH

Endogenously Generated Omega-3 Fatty Acids Attenuate Vascular Inflammation and Neointimal Hyperplasia by Interaction With Free Fatty Acid Receptor 4 in Mice

Xinzhi Li, PhD; Laurel L. Ballantyne, BSc; Xinghui Che, BSc; Jeffrey D. Mewburn, BSc; Jing X. Kang, MD, PhD; Robert M. Barkley, PhD; Robert C. Murphy, PhD; Ying Yu, PhD; Colin D. Funk, PhD

***Background*—**Omega-3 polyunsaturated fatty acids (ω3 PUFAs) suppress inflammation through activation of free fatty acid receptor 4 (FFAR4), but this pathway has not been explored in the context of cardiovascular disease. We aimed to elucidate the involvement of FFAR4 activation by ω3 PUFAs in the process of vascular inflammation and neointimal hyperplasia in mice.

***Methods and Results*—**We used mice with disruption of FFAR4 (*Ffar4*$^{-/-}$), along with a strain that synthesizes high levels of ω3 PUFAs (*fat-1*) and a group of crossed mice (*Ffar4*$^{-/-}$/*fat-1*), to elucidate the role of FFAR4 in vascular dysfunction using acute and chronic thrombosis/vascular remodeling models. The presence of FFAR4 in vascular-associated cells including perivascular adipocytes and macrophages, but not platelets, was demonstrated. ω3 PUFAs endogenously generated in *fat-1* mice (n=9), but not in compound *Ffar4*$^{-/-}$/*fat-1* mice (n=9), attenuated femoral arterial thrombosis induced by $FeCl_3$. Neointimal hyperplasia and vascular inflammation in the common carotid artery were significantly curtailed 4 weeks after $FeCl_3$ injury in *fat-1* mice (n=6). This included greater luminal diameter and enhanced blood flow, reduced intima:media ratio, and diminished macrophage infiltration in the vasculature and perivascular adipose tissue compared with control mice. These effects were attenuated in the *Ffar4*$^{-/-}$/*fat-1* mice.

***Conclusions*—**These results indicate that ω3 PUFAs mitigate vascular inflammation, arterial thrombus formation, and neointimal hyperplasia by interaction with FFAR4 in mice. Moreover, the ω3 PUFA–FFAR4 pathway decreases inflammatory responses with dampened macrophage transmigration and infiltration. **(*J Am Heart Assoc*. 2015;4:e001856 doi: 10.1161/JAHA.115.001856)**

Key Words: adipose tissue • fatty acids • inflammation • omega-3 fatty acid receptor • transgenic model

Since the seminal observations in Greenland Eskimos published in the 1970s[1,2] on the cardiovascular benefits of diets enriched in fish containing omega-3 polyunsaturated fatty acids (ω3 PUFAs; eg, eicosapentaenoic acid [EPA] and docosahexaenoic acid [DHA]), understanding of the mechanisms of the health benefits of ω3 PUFAs have been sought. Over the ensuing years, studies have revealed that they can be cardioprotective,[3] anti-inflammatory,[4] and anti-carcinogenic.[5] ω3 PUFAs may reduce the risk of cardiovascular disease by means of beneficial effects on arrhythmic, atherosclerotic, inflammatory, and thrombotic processes.[6] The antithrombotic effects of EPA and DHA could result from the ability of these fatty acids to reduce arachidonic acid oxidation and synthesis of prostaglandins and thromboxane.[7] They may attenuate balloon injury–induced vascular neointima hyperplasia[8] in mice, possibly by inhibition of vascular smooth muscle cell proliferation.[9] Some recent epidemiological studies,[10–12] however, challenged the dogma that ω3 PUFAs reduce cardiovascular events, in stark contrast to the compelling early studies.[2] Speculation about the reason for these discrepancies is rampant and speaks to the need for more mechanistic insight into the actions by which ω3 PUFAs may control vascular dysfunction.

Recently, free fatty acid receptor 4 (FFAR4; formerly G protein-coupled receptor 120, GPR120), a receptor/sensor

From the Department of Biomedical and Molecular Sciences (X.L., L.L.B., X.C., C.D.F.) and Cancer Research Institute (J.D.M.), Queen's University, Kingston, Ontario, Canada; Key Laboratory of Nutrition and Metabolism, Institute for Nutritional Sciences, Shanghai Institutes for Biological Sciences, Chinese Academy of Sciences, Shanghai, China (Y.Y.); Laboratory for Lipid Medicine and Technology, Massachusetts General Hospital and Harvard Medical School, Boston, MA (J.X.K.); Department of Pharmacology, University of Colorado Denver, Aurora, CO (R.M.B., R.C.M.).

Correspondence to: Colin D. Funk, PhD, Department of Biomedical and Molecular Sciences, Queen's University, Botterell Hall, Room 433, 18 Stuart St., Kingston, Ontario, Canada K7L 3N6. E-mail: funkc@queensu.ca

Received January 27, 2015; accepted March 20, 2015.

for long-chain fatty acids including ω3 PUFAs, has attracted widespread attention based on evidence of FFAR4 mediating anti-inflammatory and insulin-sensitizing activity.[13] Animal models and human studies show that FFAR4 modulates food intake and body weight gain, adipocyte differentiation, and obesity.[14] Consequently, many reports have focused on the antiobesity and chronic inflammation-dampening effects elicited by activation of FFAR4.[15–18.]

Obesity-related cardiovascular disorders involve complex inflammatory cascades with infiltration of monocytes and macrophages and other inflammatory cells and initiation of neointimal hyperplasia.[19,20] Adipose tissues play important roles in the crosstalk with their neighbor organs, including blood vessels, kidney, and heart, with perivascular adipose tissue (PVAT) being important in vascular inflammation.[21] Early evidence has shown that FFAR4 is expressed in both macrophages and adipose tissue[13,14]; therefore, targeting FFAR4 to ameliorate inflammation and obesity, and perhaps also vascular diseases, is expected as a potential novel therapeutic strategy.

Surprisingly, very little has been published related to the cardiovascular effects relevant to ω3 PUFA–FFAR4 signaling. In the present study, we aimed to elucidate the involvement of FFAR4 activation by ω3 PUFAs in the process of arterial thrombosis and neointimal hyperplasia in mice. We used transgenic *fat-1* mice, capable of generating significant amounts of ω3 PUFAs from ω6 PUFAs,[22] and compound *fat-1*/FFAR4 knockout mice together with laser Doppler and ultrasound imaging across several cardiovascular injury models to examine the role of the ω3 PUFA–FFAR4 pathway. We found that endogenously generated ω3 fatty acids in *fat-1* mice mitigate arterial damage–initiated thrombus formation and neointimal hyperplasia and may exert beneficial cardioprotective actions by activation of FFAR4.

Methods

Generation and Breeding of FFAR4 Knockout and *fat-1* Mice

The *Ffar4*$^{-/-}$ mouse strain on a C57BL/6 genetic background used for this research project was created from an embryonic stem cell clone (15078A-A9) generated by Regeneron Pharmaceuticals, Inc and made into live mice by the Knockout Mouse Project Repository and the Mouse Biology Program at the University of California Davis. Methods used to create the VelociGene targeted alleles have been published.[23] Briefly, the *Ffar4* gene, including exons 1 to 3, was disrupted by gene targeting with a vector (ZEN-UB1) containing a reporter *lacZ* and a selection cassette (neomycin) driven by the promoter from the human ubiquitin C gene and flanked with 2 lox*P* sites.

Fat-1 breeders on a C57BL/6 background were provided by Dr Jing X. Kang (Harvard Medical School). In this study, *fat-1* mice were crossbred with FFAR4 knockout mice over 2 generations to obtain the compound *Ffar4*$^{-/-}$*/fat-1* hemizygous transgenic mice. The *fat-1* and *Ffar4* genotypes of each mouse were confirmed by polymerase chain reaction (PCR) using tail genomic DNA after weaning and again after euthanization. Primers used for FFAR4 knockout mice: common reverse, 5′-CTGTAGGGTGCTACAGTACTC-3′; wild type (WT)-specific forward, 5′-AATACCCGACTTCCAACAGC-3′ and targeted allele-specific forward, 5′-GCAGCCTCTGTTCCA CATACA-3′. These primers amplified bands of 850 base pairs from the targeted *Ffar4*$^{-/-}$ homozygous and 733 base pairs from *Ffar4*$^{+/+}$ (WT) alleles. The *fat-1* mouse genotyping primers used were 5′-CTGCACCACGCCTTCACCAACC-3′ and 5′-CACAGCAGCAGATTCCAGAGATT-3′. The fragment amplified with these primers was 250 base pairs in size.[24]

All mice were housed ≤4 mice per cage in a temperature- and humidity-controlled animal facility with a 12-hour light/dark cycle. Food and water were available ad libitum. All mice were maintained after weaning on a modified AIN-76A rodent diet (D11122101; Research Diets) containing 10% corn oil (22 kcal percentage of fat), which is high in linoleic acid (18:2 ω6) and has trace levels of α-linolenic acid (18:3 ω3). Both male and female 4-week-old mice were housed individually, and body weight and food intake were recorded twice weekly until mice were 12 weeks old. Food intake per mouse per day was averaged weekly over the course of 8 weeks. In another set of experiments, mice (18 to 22 weeks old) maintained on the modified diet were euthanized. The liver and white adipose tissues from subcutaneous (extending from the dorsolumbar area to the inguinal area), epididymal (male), periuterine (female), and perirenal regions were excised and weighed. All procedures for animal experimentation were undertaken in accordance with the principles and guidelines of the Canadian Council on Animal Care and were approved by the Queen's University animal care committee.

X-Gal Staining

Expression of active β-galactosidase from the *lacZ* gene driven by the *Ffar4* promoter allows the use of 5-bromo-4-chloro-3-indolyl-beta-D-galactopyranoside (X-gal) staining as a surrogate for native sites of FFAR4 expression in *Ffar4*$^{-/-}$ mice. Stomach, small intestine, colon, adipose tissues (subcutaneous and perirenal), perivascular adipose tissue (PVAT) surrounding the abdominal aorta, and brown adipose tissue (interscapular) from both WT and *Ffar4*$^{-/-}$ mice were dissected and fixed for 15 minutes in cold 2% paraformaldehyde/0.2% glutaraldehyde. X-gal staining was performed at 37°C in PBS containing 2 mmol/L magnesium chloride, 5 mmol/L potassium ferrocyanide trihydrate, 5 mmol/L

potassium ferricyanide crystalline, 1 mg/mL X-gal, and 2.5% dimethyl sulfoxide. WT tissues were used as negative controls for endogenous β-galactosidase activity. Color changes were observed every 30 minutes for the first 5 hours and then left overnight. Stained tissues were rinsed in PBS and then photographed using a digital camera (Q-Color5; Olympus Corp) under the stereomicroscope (MZ16; Leica Microsystems Pty Ltd).

In the case of X-gal staining of lung sections and arteries (carotid, thoracic, and abdominal aortic), tissues were fixed for 10 to 15 minutes and snap frozen in optimal cutting temperature medium with liquid nitrogen. Sections were cut and stained with X-gal overnight in a humidified chamber at 37°C. After brief rinses with PBS and distilled water, sections were counterstained with Nuclear Fast Red, then air dried and mounted with Cytoseal 60 medium (Richard-Allan Scientific). Visualization was performed with a microscope (Leica).

Determination of ω3/ω6 Fatty Acids

Fatty acid profiles of 12-week-old mouse tails were analyzed by gas chromatography, as described previously.[24,25] Briefly, each mouse tail sample (≈0.5 cm) was homogenized and extracted, and fatty acid methyl esters were prepared using 14% boron trifluoride in methanol. Sealed samples were stored at −20°C until further analysis was performed. Gas chromatography (Shimadzu GC-17A) with flame ionization detection and capillary column (HP-Innowax, 19091N-113; HP Agilent) was used to analyze fatty acid methyl esters. Gas chromatography standard (GLC 461; Nu-Chekprep Inc) was used to identify fatty acid methyl esters. Values are expressed as an area percentage of total measured fatty acids.

After mice were euthanized by CO_2, blood was collected by cardiac puncture and allowed to coagulate at room temperature. Following overnight storage at 4°C, serum was obtained by centrifugation at 2000*g* for 5 minutes and kept at −80°C. Fatty acids including arachidonic acid, EPA, and DHA in serum were determined by liquid chromatography–mass spectrometry analysis, as described previously.[26,27]

Femoral Artery Thrombosis and Laser Doppler Tissue Perfusion Imaging

Mice aged 10 to 12 weeks were used, and hair was gently removed using a combination of mechanical shaving and chemical depilation the day before surgery. Briefly, the left femoral artery was exposed by blunted dissection under ketamine (150 mg/kg) and xylazine (10 mg/kg, intraperitoneal) anesthesia. A piece of filter paper (1×3 mm) soaked in 10% $FeCl_3$ was applied in contact with the adventitial surface of the vessel. After 5-minute exposure, the filter paper was removed, and the vessel was washed with sterile normal saline. A MoorLDI laser Doppler imager (Moor Instruments) was used to measure the relative perfusion units in hind limb before (preinjury) and after surgery (postinjury at 0, 30, 60, and 90 minutes).[28,29] The mice were put on a warm pad during this process, under anesthesia, and were euthanized by cervical dislocation immediately after conclusion of the experiment when the animals were still under deep anesthesia. We assessed the mean blood perfusion units in comparison with the nonischemic limb (right) from the same animal to minimize positional and uncontrollable field differences. Mean relative perfusion units for the ischemic limb (left) were measured in an offline mode and are presented as percentages relative to the preinjury RFU.

Chronic $FeCl_3$ Injury Model and Ultrasound Examination of Common Carotid Artery

The right common carotid artery (CCA) injury was induced by $FeCl_3$, as described previously with some modification.[30,31] Briefly, analgesia was administered (20 mg/kg tramadol [Ultram; Chiron AS]) at least 1 hour prior to surgery in mice aged 8 to 10 weeks. Mice were then anesthetized with 1% isoflurane by nose cone. The right CCA was exposed with minimal dissection. A 1×3-mm piece of filter paper soaked in 5% $FeCl_3$ solution was placed on the adventitia of the CCA for 5 minutes. The external surface of the artery was then washed with normal saline, and the skin was closed and sutured, followed by subcutaneous administration of 1.0 mL of warm normal saline solution. Mice were returned to their cages once fully mobile. The entire procedure was performed on a heated pad. All animals recovered and showed no signs of a stroke. Postoperative care, including separate caging and continuous monitoring, was provided.

The carotid artery ultrasound examination was performed by a Vevo 770 in vivo microimaging system (VisualSonics). Ultrasound images were obtained by an RMV 704 scanhead in mice 1 day prior to surgery (as a baseline) and followed by weekly ultrasound measurements for 4 weeks after surgery. Mice were anaesthetized using 1% isoflurane delivered by nose cone. Hair around the neck was removed using a combination of mechanical shaving and chemical depilation, and mice were placed on a heated platform in a supine position. Rectal temperature and electrocardiogram were monitored throughout the procedure. The B-mode image was used as a guide to obtain M-mode and pulsed wave Doppler–mode images. Mean systolic luminal diameter of the right CCA was measured at ≈1 mm below the carotid bifurcation using the M-mode image, whereas the flow–velocity curve was measured with the pulsed wave Doppler–mode image. From the flow–velocity curve, mean velocity was obtained. Blood flow (mm^3/s) was calculated as mean velocity$\times\pi r^2\times\cos\theta$ (r indicates radius equal to mean luminal

diameter/2; θ indicates Doppler beam angle against the blood flow). Multiple measurements were made for each parameter, with an average of 3 to 5 cardiac cycles used for all calculations.

One day after the last ultrasound imaging (at 28 days after $FeCl_3$ injury), the mice were euthanized by CO_2 and were perfused through the left ventricle with ice-cold PBS. Both CCAs (right, affected; left, unaffected) were carefully harvested and embedded in blue frozen section compound (VWR) for immunohistochemistry and for hematoxylin and eosin staining.

Histological and Immunofluorescence Staining

CCAs were cut (6 μm) and histologically stained routinely with hematoxylin and eosin for morphological analysis. Stained sections were photographed using a microscope (Leica). As described previously,[30,31] the luminal, intimal, and medial areas were calculated for each section using Image-Pro Plus software (Media Cybernetics). The intimal area was calculated as the area encircled by internal elastic lamina minus the luminal area. The medial area was calculated as the area encircled by the external elastic lamina minus intimal area. The intima:media ratio was calculated as the intimal area divided by the medial area. The area values from 3 artery sections were used to obtain average values. Intima: media ratio was used as the main parameter to evaluate neointimal hyperplasia. Immunofluorescence staining was performed by incubation of sections with primary antibodies directed against mouse CD68 (1:100, 137001; BioLegend), CD31 (fluorescein isothiocyanate conjugated, 1:200, 102506; BioLegend), and α-smooth muscle actin (fluorescein isothiocyanate conjugated, 1:200, F3777; Sigma-Aldrich), as described previously.[32,33] Slides were then dehydrated, mounted with ProLong Gold antifade reagent with DAPI (Invitrogen), and stored at room temperature until analysis. Visualization was performed with a fluorescent microscope (Leica); photomicrographs (×20, ×40 objective) were recorded, and quantification of positively stained cells was conducted with Image-Pro Plus software (Media Cybernetics). All specimens were analyzed by an investigator blinded to the study design.

RNA Extraction and Quantitative or Reverse Transcription PCR

Aortic smooth muscle from 3 mice of each strain was dissected and pooled, as per the protocol used previously in our laboratory.[34] Peripheral lymphocytes were isolated by Lympholyte medium (CL5110; Cedarlane). WT lung endothelial cells were isolated by enzymatic digestion[35] and grown in endothelial cell basal medium-2 (CC3156; Lonza) with the supplement of growth factors (CC-4147; Lonza). Endothelial cells were then subjected to fluorescence-activated cell sorting using a fluorescein isothiocyanate–conjugated *Griffonia simplicifolia* IB_4 isolectin antibody with a Beckman Coulter EPICS Altra flow cytometer.[35] Total cellular RNA was extracted from various tissues or cells using the RNeasy Mini Kit (catalog no. 74104; Qiagen), according to the manufacturer's instructions. After treatment with DNase I, RNA quantity was assessed using a Nanodrop N-1000 spectrophotometer (Nanodrop).[36] Total RNA (1 μg) was reverse transcribed to cDNA using the iScript kit (BioRad), according to the manufacturer's protocol. Quantitative PCR was performed using a thermal cycler (Applied Biosystems Model 7500) with SYBR Green PCR master mix (BioRad). GAPDH was used as a control housekeeping gene. Melting curves were performed on completion of the cycles to ensure absence of nonspecific products. Oligonucleotide primers were acquired from Eurofins MWG Operon and are listed in Table 1. Data were calculated using the $2^{-\Delta\Delta CT}$ method and are presented as fold-induction of transcripts for target genes normalized to GAPDH, with respect to controls.[15]

Data Analysis

Data are expressed as mean±SEM. The Kolmogorov-Smirnov test was used as a normality test. One-way ANOVA analysis was used for normally distributed variables, and the Tukey honestly significant difference post hoc comparisons were conducted when the ANOVA indicated a significant difference among the compared means. Nonparametric Kruskal–Wallis tests were used for non-normally distributed variables. Repeated measures of postbaseline body weight, food consumption, relative blood flow in hind limbs, and luminal diameter/blood flow of right CCA were analyzed by use of a general linear model followed by Tukey honestly significant difference post hoc comparisons. Tests were 2-tailed, and values of $P<0.05$ were considered statistically significant. The statistical analysis was performed with IBM SPSS Statistics 19 software (IBM Corporation), and the data were plotted by GraphPad Prism 6 software (GraphPad).

Table 1. Primers Used in Quantitative Real-Time or Reverse Transcription Polymerase Chain Reactions

Gene	Protein	Primers, 5′ to 3′	AP (bp)
Gapdh	GAPDH	F: CATGGCCTTCCGTGTTCCTA R: ATGCCTGCTTCACCACCTTCT	106
Ffar4	FFAR4	F: CAACCGCATAGGAGAAATCT R: GGACTCCACATGATGAAGAA	240

Gene names, primer sequences, and AP sizes in base pairs for primers used in this study. AP indicates amplicon; bp, base pairs.

Results

Generation and Characterization of FFAR4 Knockout Mice

To create FFAR4 knockout mice, the *Ffar4* gene was disrupted by gene targeting with a vector containing a reporter *lacZ* and a selection cassette (neomycin) driven by the promoter from the human ubiquitin C gene and flanked with 2 lox*P* sites[23] (Figure 1A). Using reverse transcription PCR, quantitative PCR, and X-gal staining from the β-galactosidase reporter, which represents native sites of FFAR4 expression, we found that FFAR4 is highly expressed in gastrointestinal tract, lung, and various adipose tissues and resident peritoneal macrophages (Figure 1C and 1D), consistent with previously published results.[14,37]

FFAR4 knockout mice were crossbred with *fat-1* mice[22] to obtain compound *Ffar4*$^{-/-}$*/fat-1* mice. Gas chromatography and liquid chromatography–mass spectrometry results showed a shift in the ω6/ω3 PUFA ratio in transgenic *fat-1* and compound *Ffar4*$^{-/-}$*/fat-1* mice compared with mice without the *fat-1* transgene (Table 2; Figure 2) when they were placed on a special diet rich in ω6 fatty acids. The results indicated lower levels of ω6 polyunsaturated acids (arachidonic acid) and more abundant ω3 fatty acids (α-linolenic acid, DHA, EPA, and docosapentaenoic acid) in transgenic *fat-1* mice (both *fat-1* and *Ffar4*$^{-/-}$*/fat-1* mice). The transgene *fat-1* enables endogenous ω3 PUFA synthesis from ω6 PUFA via a ω3 fatty-acid desaturase enzyme[38]; however, there was no difference in fatty acid profiles between WT and *Ffar4*$^{-/-}$ mice or between *fat-1* and *Ffar4*$^{-/-}$*/fat-1* mice. This indicates that any phenotypic differences observed between *fat-1* and *Ffar4*$^{-/-}$*/fat-1* mice are most likely the result of loss of murine FFAR4 expression. We carried out all subsequent studies using 4 strains of mice: (1) control C57BL/6, WT; (2) mice capable of forming significant amounts of ω3 PUFA, *fat-1*; (3) FFAR4 knockout, *Ffar4*$^{-/-}$; and (4) compound *Ffar4*$^{-/-}$*/fat-1*.

Body weight was similar in both WT and FFAR4-deficient groups of mice on the ω6 PUFA-rich diet; however, the body weight of mice with the *fat-1* transgene (*fat-1* and compound *Ffar4*$^{-/-}$*/fat-1*) versus without *fat-1* (WT and *Ffar4*$^{-/-}$) was slightly less in mice aged ≈6 to 10 weeks but not in old mice, aged ≈20 weeks (Figure 3A, 3B, and 3E), which is consistent with a previous report in *fat-1* mice.[39] On the ω6 PUFA diet, no significant differences in food intake were observed between the 4 groups of male and female mice (Figure 3C and 3D).

FFAR4 plays a critical role in adipose tissue homeostasis including regulation of adipocyte differentiation and lipogenesis.[14] We measured the weights of several adipose depots, which showed that white adipose tissues (subcutaneous, epididymal/periuterine, perirenal) were heavier in older FFAR4 mutant mice (aged 18 to 22 weeks) than those in their counterparts, with no difference in liver weights when fed the ω6 PUFA diet (Figure 3F). This is consistent with a previous report in mice fed a high-fat diet.[14]

FFAR4 is Expressed in Both Vascular and Perivascular Cells

FFAR4 expression was observed previously in adipose tissue macrophages, adipocytes, Kupffer cells, monocytic RAW 264.7 cells, and enteroendocrine L cells[13]; however, FFAR4 expression in cardiovascular disease–associated settings within smooth muscle cells and perivascular adipose tissue has not been reported to date. Our quantitative PCR results demonstrated relative mRNA expression in various tissues and cells, with a rank order of PVAT, macrophage, lymphocyte, vascular smooth muscle cells, and then lung endothelial cells (Figure 4A). X-gal staining of lung sections revealed that FFAR4 is seen in epithelial cells of bronchi and bronchioles but not in accompanying vessels (Figure 4B). Using reporter gene staining, FFAR4 is also highly expressed in PVAT of carotid, thoracic, and abdominal aorta arteries, with much weaker expression in vascular smooth muscle cells and lymophocytes (Figure 4C). FFAR4 was not found in platelets using X-gal staining and Western blot analysis (data not shown). Consequently, these vascular-specific FFAR4 expression patterns should provide insight into how FFAR4 regulates the complex interactions between vascular and perivascular cells (adipocytes and macrophages) in the context of inflammation.

ω3 Fatty Acids Mitigate Femoral Artery Thrombosis via FFAR4

Localized vascular (femoral artery) application of $FeCl_3$ causes major oxidative stress with the generation of free radicals, leading to lipid peroxidation, destruction of endothelial cells, and occlusive thrombus formation.[40] Initiation of thrombus caused a significant decrease in blood flow of the affected left hind limb in all 4 groups. WT mice (n=9) showed a decrease (51±8% versus preinjury) in blood flow at 30 minutes after $FeCl_3$ injury, and this was maintained until the end of the experiment at 90 minutes (39±7% versus preinjury). Postinjury blood flow in *fat-1* mice (n=9) dropped less compared with WT mice at 60 and 90 minutes, with blood flow greater relative to WT littermates (74±13% and 80±13%, respectively; $P<0.05$ versus WT) (Figure 5). Change in blood flow was not statistically significant versus WT in *Ffar4*$^{-/-}$ mice (n=7), and flow in *Ffar4*$^{-/-}$*/fat-1* (n=9) mice decreased after 30 minutes and was maintained until 90 minutes but showed a significant decline at 90 minutes compared with *fat-1* mice (both $P<0.05$). Blood flow did not vary among any of the

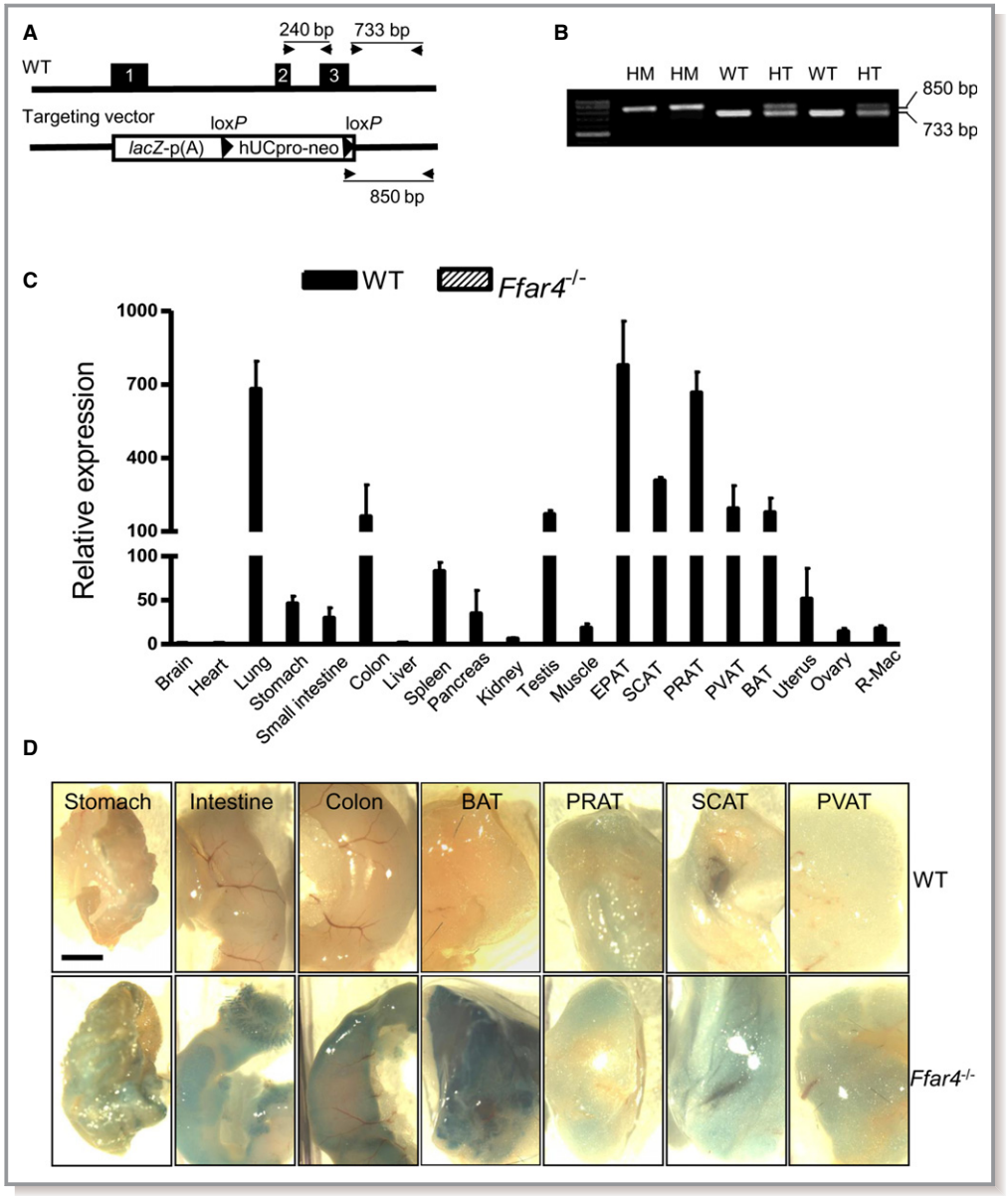

Figure 1. Generation of *Ffar4*$^{-/-}$ mouse strain and tissue distribution of FFAR4. A, Strategy to generate *Ffar4*$^{-/-}$ mice. The *Ffar4* gene, including exons 1 to 3 (filled boxes), was disrupted by gene targeting with a vector containing a reporter *lacZ* and a selection cassette (neomycin) driven by the promoter from the hUbCpro gene and flanked with 2 lox*P* sites. p (A), poly (A). B, PCR genotyping of tail biopsies from *Ffar4*$^{+/+}$ (WT, 733 bp), *Ffar4*$^{-/-}$ HM (850 bp), or *Ffar4*$^{+/-}$ HT mice with both alleles. Locations of primers are seen in (A). C, Real time quantitative reverse transcription PCR of FFAR4 mRNA expression in mice. Values are given as mean±SEM, n=3. D, X-gal staining of whole-mount mouse tissues. Scale bar indicates 2 mm. BAT indicates brown adipose tissue (interscapular); bp, base pairs; EPAT, epididymal adipose tissue; HM, homozygous; HT, heterozygous; hUbCpro, human ubiquitin C; neo, neomycin; PCR, polymerase chain reaction; PRAT, perirenal adipose tissue; PVAT, perivascular adipose tissue (around abdominal aorta); R-Mac, resident peritoneal macrophage; SCAT, subcutaneous adipose tissue (inguinal); WT, wild type; X-gal, 5-bromo-4-chloro-3-indolyl-beta-D-galactopyranoside.

experimental groups in the nonischemic right limb. These results provide evidence that endogenously generated ω3 fatty acids mitigate arterial damage–initiated thrombus formation and may exert beneficial cardioprotective actions via activation of FFAR4.

FFAR4 Interplays With ω3 Fatty Acids to Suppress Neointimal Hyperplasia

Next, we investigated the effects of ω3 fatty acids on long-term $FeCl_3$ arterial damage–induced vascular inflammation

Table 2. ω6 and ω3 Fatty Acid Composition in Tails of Mice

	WT (n=6)	*fat-1* (n=5)	*Ffar4*$^{-/-}$ (n=6)	*Ffar4*$^{-/-}$/*fat-1* (n=6)
C18:2 (ω6; LA)	19.7±2.7	18.3±2.1	19.0±1.8	13.9±1.7
C18:3 (ω6; GLA)	0.1±0	0.1±0	0.2±0.1	0.1±0
C20:4 (ω6; AA)	4.5±0.8	0.5±0.1*	4.8±0.7	0.7±0.1*†
C18:3 (ω3; ALA)	0.1±0	1.6±0.1*	0.1±0	1.9±0.1*†
C20:5 (ω3; EPA)	ND	1.1±0.2	ND	1.3±0.1
C22:5 (ω3; DPA)	0.2±0	0.8±0.1*	0.1±0.1	0.9±0.1*†
C22:6 (ω3; DHA)	0.8±0.1	1.4±0.1*	0.9±0.2	1.3±0.1*
ω6 PUFAs	26.0±1.9	19.6±2.0**	25.9±1.3	16.0±1.7*†
ω3 PUFAs	1.0±0.1	4.9±0.3*	1.1±0.3	5.5±0.2*†
ω6/ω3‡	27.4±4.3	4.1±0.7*	28.8±4.5	2.9±0.3*†

Tails of mice were collected for analysis of fatty acids by gas chromatography flame ionization detection. Values, which are expressed as an area percentage of total measured fatty acids, are shown as mean±SEM. AA indicates arachidonic acid; ALA, α-linolenic acid; DHA, docosahexaenoic acid; EPA, eicosapentaenoic acid; GLA, γ-linolenic acid; LA, linoleic acid; ND, not detectable; PUFAs, polyunsaturated fatty acids; WT, wild type.
*P<0.01 compared with WT.
**P<0.05 compared with WT.
†P<0.01 compared with *Ffar4*$^{-/-}$, determined by 1-way ANOVA post hoc analysis.
‡The mean of the ratios of 2 variables is not exactly equal to the ratio of their means.

and neointimal hyperplasia in the CCA. Ultrasonographic assessment at the bifurcation of the right carotid artery showed that luminal diameter did not differ significantly between the 4 groups at baseline; however, the luminal diameter in WT mice decreased significantly at 1 week after injury. This phenomenon persisted in both *Ffar4*$^{-/-}$ and *Ffar4*$^{-/-}$/*fat-1* mice from 1 to 4 weeks but not in *fat-1* mice, whose CCA luminal diameter was greater than that of WT and *Ffar4*$^{-/-}$/*fat-1* mice (P<0.05) (Figure 6A and 6C). In accordance with luminal diameter data, blood flow detected by pulsed wave Doppler of *fat-1* mice showed significant elevation versus mice in the other 3 groups (WT, *Ffar4*$^{-/-}$, and *Ffar4*$^{-/-}$/*fat-1*) (Figure 6B and 6D). These data indicate that the absence of FFAR4 results in loss of beneficial actions exerted via ω3 PUFAs.

Representative hematoxylin and eosin–stained CCA sections of normal control vessels and $FeCl_3$-injured arteries showed distinct morphological changes at 28 days with a large neointima composed of smooth muscle cells (Figure 7A and 7B), which is consistent with a previous study.[31] A smooth muscle cell–rich neointima (α-smooth muscle actin positive) lined with CD31-positive endothelial cells was observed at 28 days after $FeCl_3$ injury in all 4 groups of mice (Figure 7C through 7E). Intima:media ratio determination, the main parameter for evaluating neointimal hyperplasia, revealed that *fat-1* mice had a lower intima:media ratio than the other 3 groups of mice (Figure 7F). This indicates that $FeCl_3$ arterial injury led to neointimal hyperplasia, which can be markedly reduced by ω3 PUFA in *fat-1* mice through an FFAR4-dependent mechanism.

ω3 Fatty Acids Dampen Vascular Inflammation Through FFAR4 Pathways

Growing evidence suggests that white PVAT (eg, surrounding carotid artery) can support vascular inflammation via macrophage accumulation and secretion of adipokines.[21,41,42] Along with the neointimal hyperplasia results, we found increased macrophage infiltration into both the neointima (Figure 8A) and the PVAT (Figure 8B) using immunohistochemistry (CD68 staining) in sections from injured CCA compared with unaffected CCA (data not shown). FFAR4 activation by ω3 PUFAs decreases adipose tissue macrophage infiltration and reduces proinflammatory gene expression.[13] Consistent with these findings, there was a substantial decrease in positively labeled macrophages in *fat-1* mice ($7\pm1/10^4$ μm^2) versus WT mice ($26\pm4/10^4$ μm^2, P<0.01), but there was no effect in *Ffar4*$^{-/-}$/*fat-1* mice (Figure 8C).

Discussion

Although it has long been accepted that ω3 PUFAs reduce the risk of cardiovascular disease,[6] some clinical studies have shown conflicting results,[11,12,43] provoking considerable debate about the efficacy of ω3 PUFAs in the management of heart disease. In this study, using a novel compound transgenic mouse model (*Ffar4*$^{-/-}$/*fat-1*) that makes ω3 PUFAs endogenously but lacks FFAR4, we found a potential mechanism involving FFAR4 signaling by which ω3 PUFAs can dampen vascular inflammation, attenuate neointimal formation, and suppress arterial thrombosis.

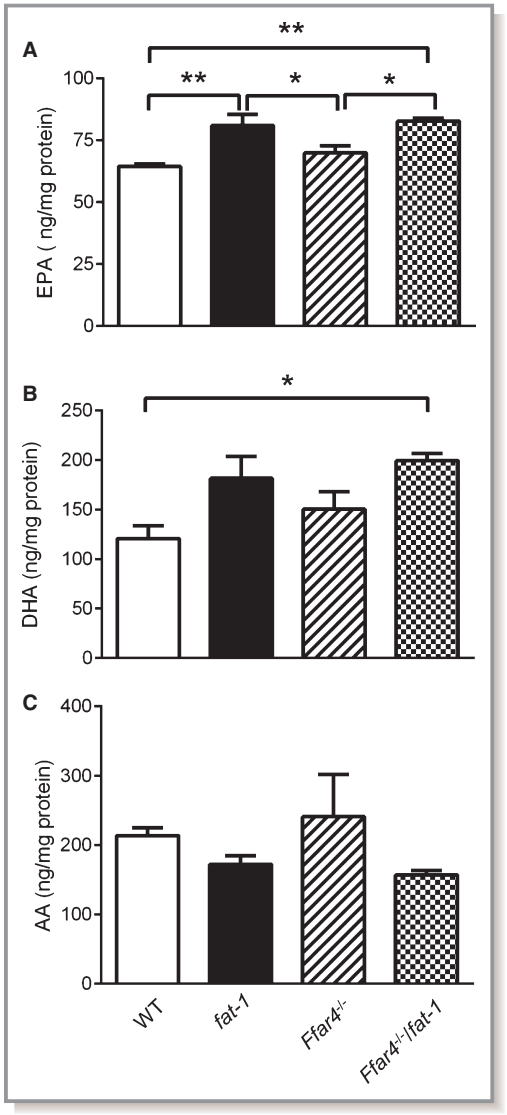

Figure 2. Measurement of fatty acids in serum of mice by liquid chromatography–mass spectrometry. A, EPA. B, DHA. C, AA. Fatty acid concentration was normalized with total serum protein content. **P*<0.05, ***P*<0.01. Values are given as mean ±SEM, n=6. AA indicates arachidonic acid; DHA, docosahexaenoic acid; EPA, eicosapentaenoic acid; WT, wild type.

For the first time, we demonstrated compelling evidence for strong FFAR4 expression in perivascular cells (adipocytes and macrophages) with weaker expression in vascular smooth muscle cells and lymphocytes and no detectable expression in platelets and endothelial cells. The high expression in PVAT and macrophages prompted us to consider the involvement of these cells in the context of an "outside-in" signaling model of vascular inflammation.

Cardiovascular inflammation, involving infiltration of monocytes and macrophages and other inflammatory cells, plays a central role in mediating obesity-related cardiovascular disorders. In this inflamed setting, PVAT is an important player in regulating vascular function in both autocrine and paracrine manners.[21] PVAT is the fat tissue surrounding blood vessels (both artery and vein)[44] that was long believed to be simply lipid-rich connective tissue, serving primarily as a supporting scaffold for blood vessels. In rodents, the mesenteric, carotid, and femoral arteries are surrounded by white adipose tissue, whereas the thoracic aorta is surrounded by brown adipose tissue, and the abdominal aorta is surrounded by beige PVAT (mixture of white and brown adipocytes).[45] Recent findings that PVAT inflammation potentially exacerbates endothelial dysfunction and atherosclerosis have led to an outside-in model of vascular injury. In this model, PVAT inflammation triggers an inward cascade from adventitia to endothelium.[46] We chose and modified the well-developed $FeCl_3$-induced artery injury model—widely used to examine thrombus formation[40]—in an attempt to maximally mimic how a PVAT-triggered cascade of events might affect ensuing vascular dysfunction. By using less $FeCl_3$ (5%) than in most thrombosis models (10%), applied directly on the adventitia with intact PVAT via soaked filter paper, the Fe^{3+} will cause major oxidative stress with the generation of reactive oxygen species and, in turn, lead to lipid peroxidation and destruction of endothelial cells.[40,47] Our data highlight that ω3 PUFAs efficiently generated in *fat-1* mice were potent to mitigate chronic $FeCl_3$-initiated vascular inflammatory cascades by reducing macrophage infiltration into the intima and PVAT and by limiting smooth muscle cell proliferation over 4 weeks. In contrast, ω3 PUFAs were nearly without effect in compound *Ffar4*$^{-/-}$*/fat-1* mice lacking the ω3 fatty acid receptor FFAR4. Along with these in vivo results, in vitro activation of FFAR4 via ω3 PUFAs prevents macrophages from propagating innate immune response by decreasing levels of proinflammatory cytokines and other lipid mediators.[15,16,18]

Researchers have transplanted different types of PVAT to address their roles during atherosclerosis[48] and neointimal hyperplasia[49]; however, transplanted PVAT disturbs the microenvironment surrounding the artery and potentially introduces immune responses to the foreign tissues. Further study will be necessary to address the precise cellular phenotypes of the PVAT in the mice used in our studies. The wire-injury model is another standard model for studying vascular remodeling[50] that follows an "inside-out" paradigm in which endothelial injury initiates inflammatory signals and recruits blood-borne immune cells to the endothelium. It will be interesting to test the mice used in our studies with this particular model.

Obesity and its associated risks of chronic inflammation result in exacerbation of cardiovascular disease. Loss of murine FFAR4 caused increased body weight and obesity-related inflammation in the context of a high-fat diet (60% fat), and this is mirrored in humans.[13,14] In line with these findings, disruption of FFAR4 likely promoted adipogenesis and

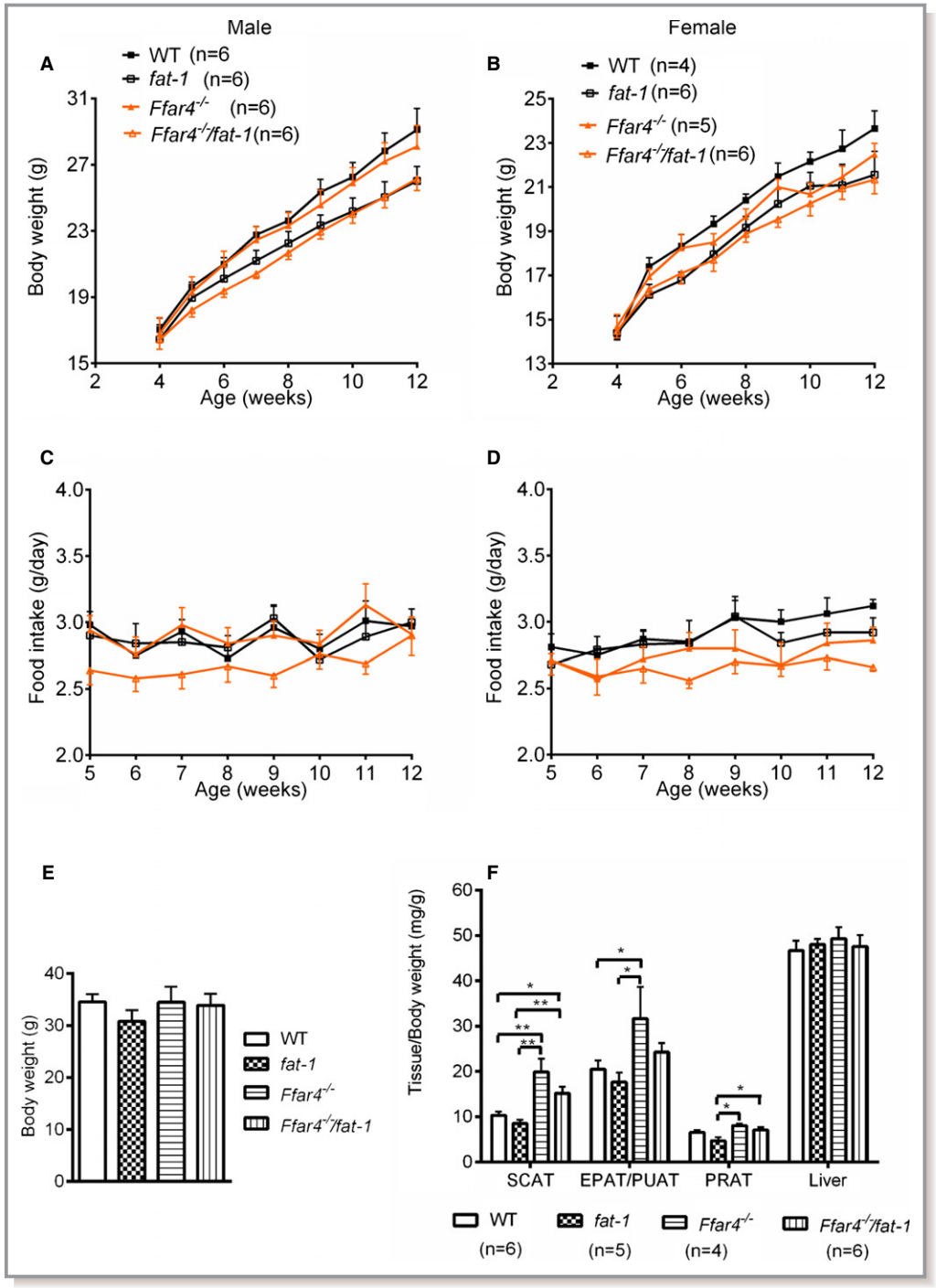

Figure 3. Body weight, tissue weight, and food intake of mice on an omega-6 (ω6) PUFA diet. A and B, Body weight changes of male and female mice were monitored twice a week when they were fed a diet rich in ω6 fatty acids (22% fat). C and D, Food consumption per day of male and female mice was averaged weekly over the course of 8 weeks. No significant differences were detected. E, There was no difference in body weights between 4 strains of mice at ≈20 weeks of age. F, Effects of an ω6 PUFA diet on liver and adipose tissue weights. **P*<0.05, ***P*<0.01. Values are given as mean±SEM, n=4 to 6 as indicated in parentheses. EPAT indicates epididymal adipose tissue; PRAT, perirenal adipose tissue; PUAT, periuterine adipose tissue; PUFA, polyunsaturated fatty acids; SCAT, subcutaneous adipose tissue (inguinal); WT, wild type.

increased fat accumulation in both epididymal and subcutaneous adipose tissues when fed with the ω6 PUFA diet with 22% fat in our studies. Interestingly, *Ffar4*$^{-/-}$ mice did not gain more weight than WT counterparts. Moreover, transgenic *fat-1* mice were slightly leaner than WT mice in early life; this may relate to the antiadipogenic effect of ω3 PUFAs during

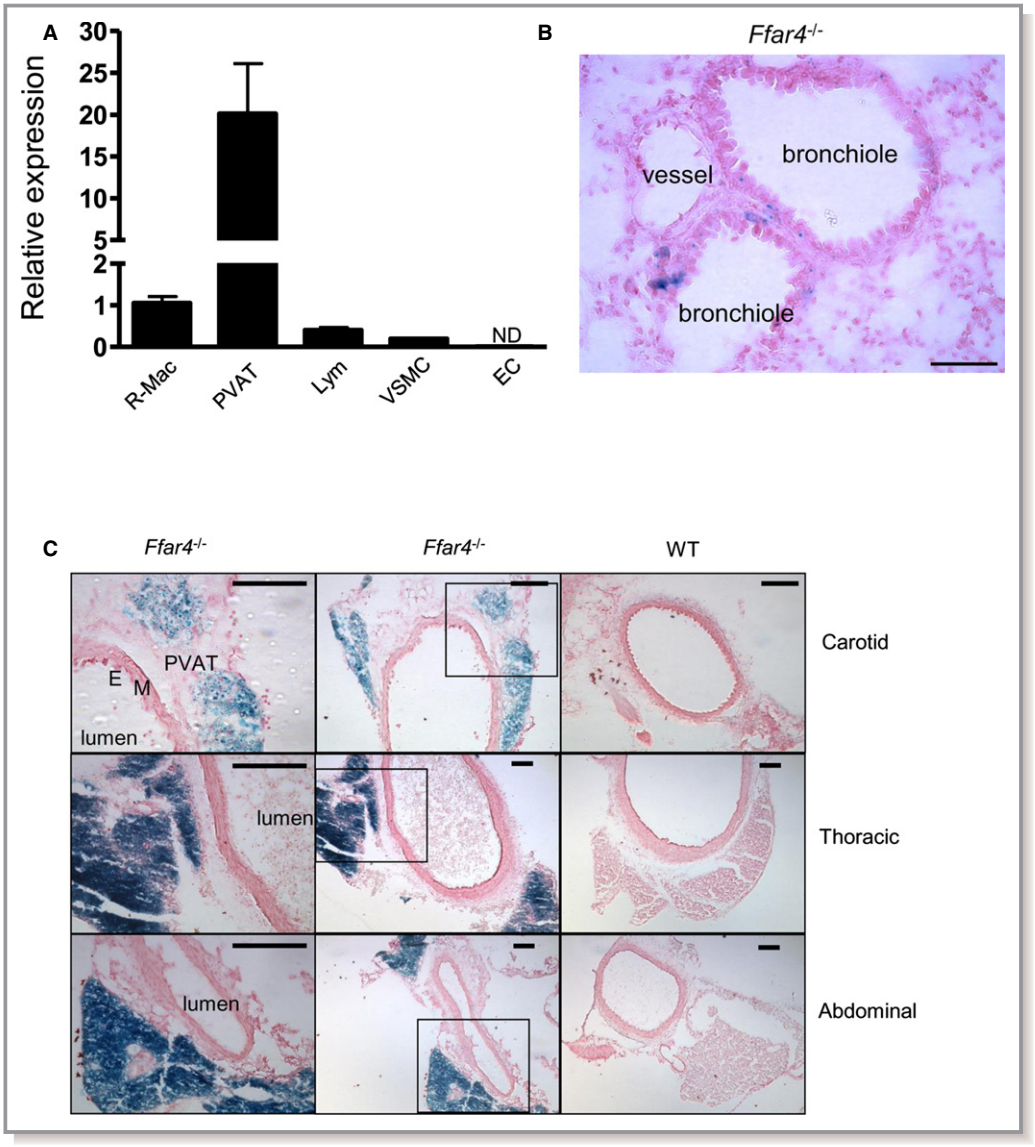

Figure 4. FFAR4 expression in both vascular and perivascular cells. A, Relative FFAR4 mRNA expression in WT mice assayed by quantitative real-time polymerase chain reaction. Values are given as mean±SEM, n=3. B, Representative bronchioles and accompanying vessel of *Ffar4*$^{-/-}$ lung. Note there is no staining in the vessel. Bar indicates 50 μm. C, FFAR4 expression in PVAT of different arteries (carotid, thoracic, and abdominal aorta). Artery sections (6 μm) were stained with X-gal and then counterstained with Nuclear Fast Red. Positive staining is seen in PVAT of all arteries but not in endothelial cells (E) or media (M). Left panels represent boxed areas of middle panels. Bars indicate 100 μm. EC indicates lung endothelial cell; Lym, circulating lymphocyte; ND, not detectable; PVAT, perivascular adipose tissue (abdominal); R-Mac, resident peritoneal macrophage; VSMC, aortic vascular smooth muscle cell; WT, wild type; X-gal, 5-bromo-4-chloro-3-indolyl-beta-D-galactopyranoside.

development of obesity.[51] A potential advantage of using transgenic *fat-1* mice and the novel strain of *Ffar4*$^{-/-}$*/fat-1* mice with the ability to directly convert ω6 to ω3 PUFA,[22] instead of supplementing diets with fish oil or ω3 PUFA for which taste issues and oxidative destruction of the diet can be problems, allows for "cleaner" assessment of this G protein-coupled receptor to vascular-specific roles played by ω3 PUFAs in the body. In this study, the ratio of ω6/ω3 PUFAs is higher in all 4 groups of mice, and the relative percentages of converted ω3 PUFAs in *fat-1* mice is likely lower than those in diet-supplementation studies.[52,53]. This result might be expected because mice were fed a ω6 PUFA diet, and the conversion efficiency of ω3 fatty acid desaturase may be limited. The ratio of ω3 PUFAs for *fat-1* and WT mice (≈5) in our study is much higher than that in fish oil–supplemented diet studies,[53] allowing us to address the effects of endogenously

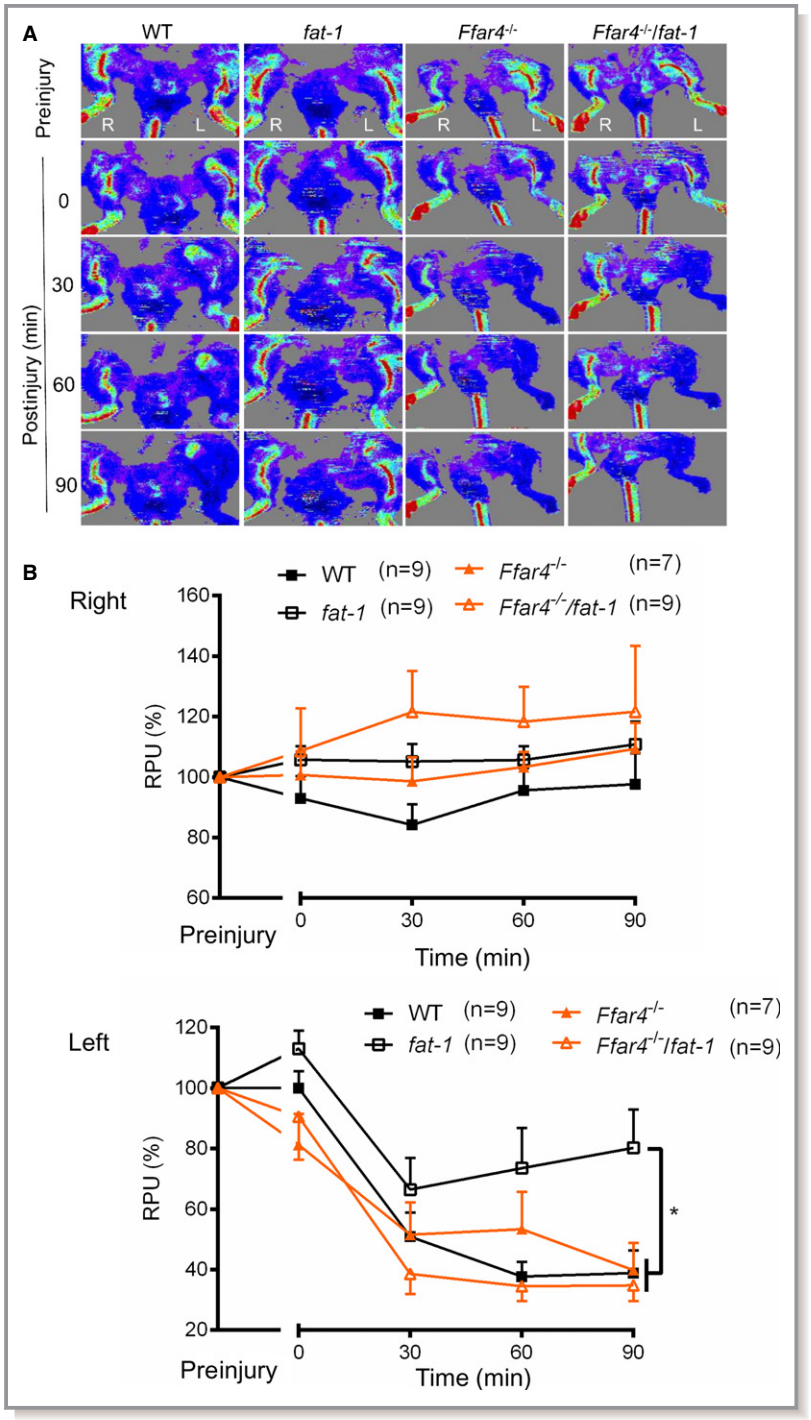

Figure 5. Knockout of FFAR4 abolishes the effects of omega-3 PUFAs on thrombus formation. A, Representative images of blood flow in hind limb scanned by laser Doppler blood perfusion imaging in an $FeCl_3$ vascular injury mouse model. Femoral artery thrombosis was induced with localized 10% $FeCl_3$ application for 5 minutes, and imaging was used to measure RPU index in hind limb before injury and after surgery (0, 30, 60, and 90 minutes after injury). Both nonischemic limb (right, R) and ischemic limb (left, L) from the same animal were assessed. B, Relative blood flow in right and left hind limb of mice. Mean RPU for the ischemic limb was measured with an offline mode and is presented as percentage relative to the preinjury RPU. *P<0.05 as determined by the "Repeated Measures in General Linear Model" of SPSS. Values are given as mean±SEM, n=7 to 9 as indicated in parentheses. PUFAs indicate polyunsaturated fatty acids; RPU, relative perfusion unit; WT, wild type.

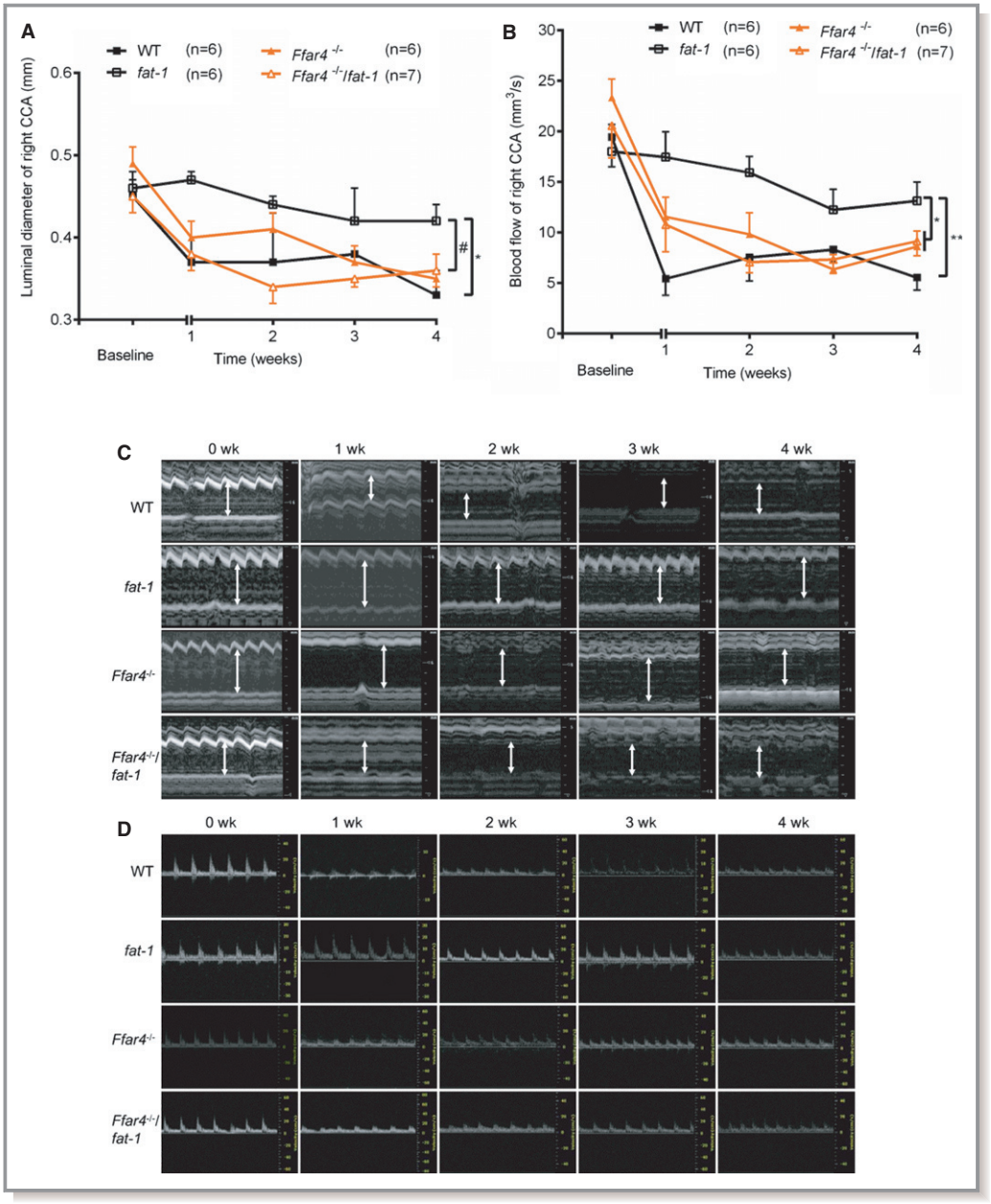

Figure 6. Ultrasonographic assessment of right carotid artery before and after $FeCl_3$ injury. A, Systolic luminal diameter of right CCA. B, Blood flow of right CCA measured by pulsed wave Doppler imaging. **P*<0.05 and ***P*<0.01 vs *fat-1*, #*P*<0.05 (*fat-1* vs *Ffar4*$^{-/-}$/*fat-1*). Values are given as mean±SEM, n=6 to 7 as indicated in parentheses. Baseline data were acquired 1 day before surgery. C, Representative images of M mode showing systolic luminal diameter measurement. D, Representative images of pulsed wave Doppler imaging of the CCA. Baseline (0 week) images were acquired 1 day before the surgery. CCA indicates common carotid artery; WT, wild type.

synthesized ω3 PUFAs in mice with the *fat-1* gene. Tissue- and cell-specific FFAR4 knockout strains should further enhance insight into the roles of this receptor in future studies.

Dietary ω3 PUFAs derived from fish oil were reported to inhibit platelet aggregation[54,55]; however, this scenario was not likely in our current studies because FFAR4 was not found in platelets. Without FFAR4 receptors on platelets, how could ω3 PUFAs exert antithrombotic effects in *fat-1* mice? We hypothesize that FFAR4 mediates inhibitory effects of ω3 PUFAs on platelet accumulation at sites of induced injury, presumably, through dampening initial stages of vascular inflammation triggered by $FeCl_3$ and reactive oxygen species but not through blocking of interactions between platelets and endothelial cells. Absence of FFAR4 in platelets does not necessarily mean the

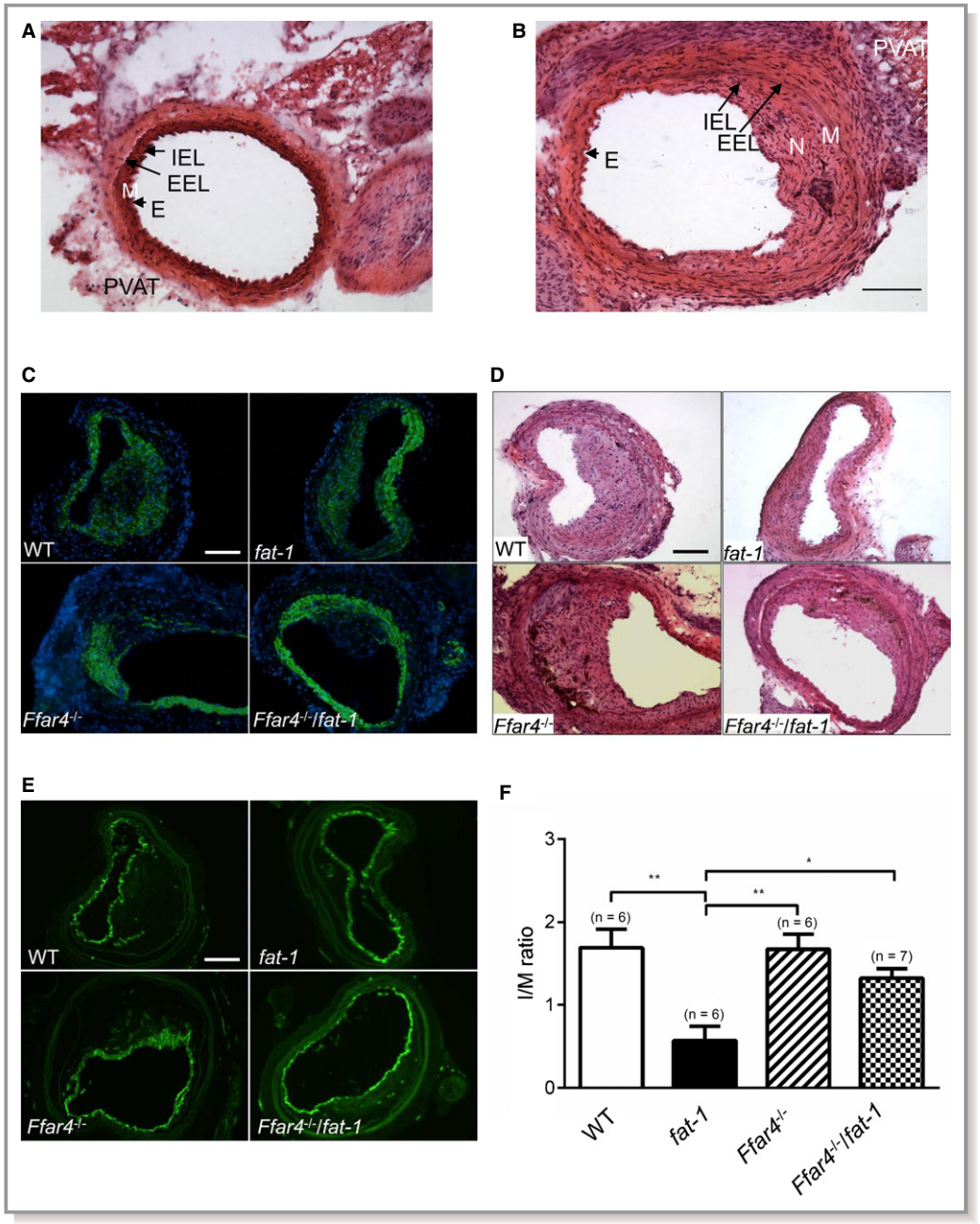

Figure 7. ω3 PUFAs via FFAR4 suppress neointimal hyperplasia. A, Representative H&E-stained images of control CCA without $FeCl_3$ injury. B, Representative image of CCA at 28 days after $FeCl_3$ injury. Bar indicates 100 μm. C, Representative images show neointima, using immunofluorescence labeling of α-smooth muscle actin (green) and nuclei (blue) in CCA of 4 strains of mice at 28 days after $FeCl_3$ injury. D, Immunostained CD31 (green) as a marker for endothelial cells. E, H&E staining. Bars indicate 100 μm. F, Calculated I/M ratio. **P*<0.05 and ***P*<0.01 determined by 1-way ANOVA post hoc analysis. Values are given as mean±SEM, n=6 to 7 as indicated in parentheses. CCA indicates common carotid artery; E, endothelial cells; EEL, external elastic lamina; H&E, hematoxylin and eosin; IEL, internal elastic lamina; I/M, intima:media; M, media; N, neointima; PUFAs, polyunsaturated fatty acids; PVAT, perivascular adipose tissue; WT, wild type.

absence of the effects of ω3 PUFAs on platelets. We showed previously that ω3 PUFA–rich fish oils favorably attenuate neointimal hyperplasia and improve cardiovascular function (platelet activity, blood pressure) by means of aspirin-triggered resolvins.[53] ω3 PUFAs can also stimulate the generation of adiponectin through interaction with specific adipocyte channels[56] and may protect blood vessels from outside-in damage in the pathogenesis of cardiovascular disorders. Furthermore, we

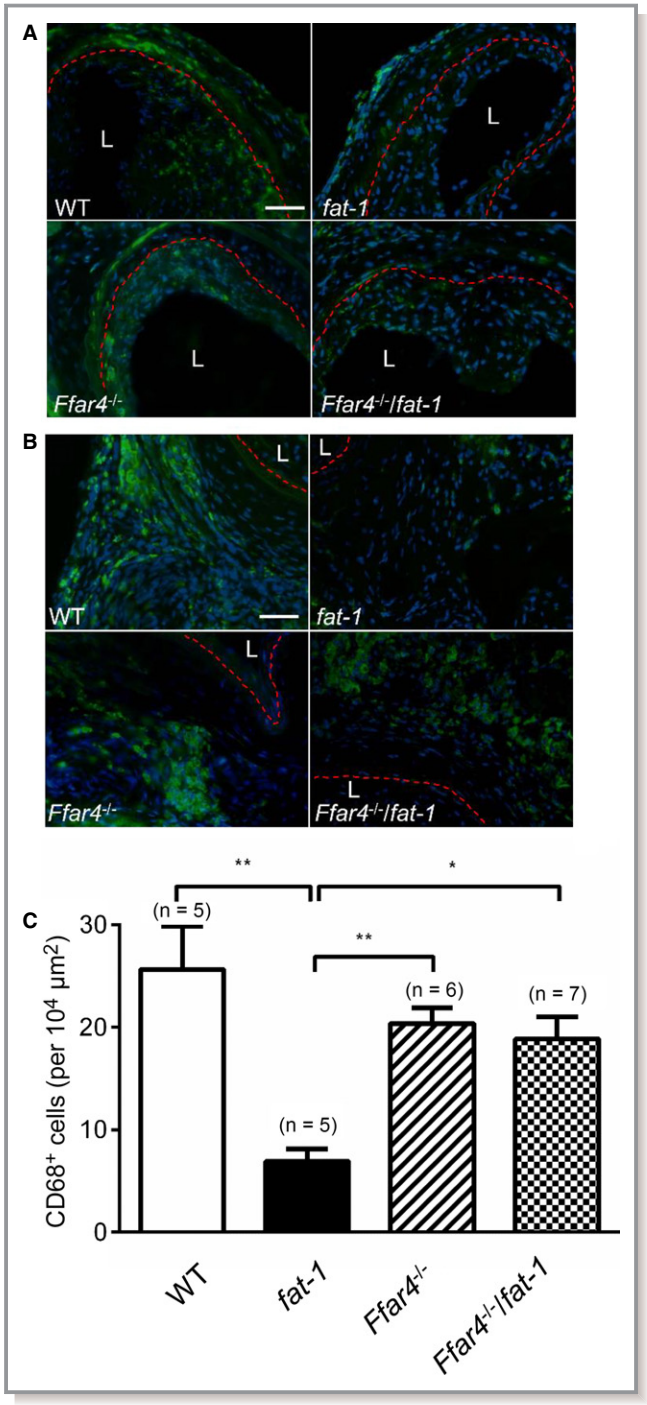

Figure 8. Anti-inflammatory effects of ω3 PUFAs are mediated by FFAR4 in vasculature and PVAT. A, Representative CD68 positively stained (fluorescein isothiocyanate, green) images in intima of 4 strains of mice. B, Representative CD68 positively stained images in PVAT of 4 strains of mice. The red lines demarcate the internal elastic lamina (A) or external elastic lamina (B), respectively. Bars indicate 50 μm. C, Number of CD68 positively stained cells in PVAT. *P<0.05 and **P<0.01 determined by 1-way ANOVA post hoc analysis. Values given as mean±SEM, n=5 to 7 as indicated in parentheses. L indicates lumen; PUFAs, polyunsaturated fatty acids; PVAT, perivascular adipose tissue; WT, wild type.

and other researchers demonstrated that ω3 PUFAs (eg, DHA), through FFAR4 signaling, alter Toll-like receptor 4–initiated pathways and limit inflammatory responses.[15–17] A highly selective FFAR4 agonist (cpdA) was recently demonstrated to improve insulin resistance and reduce inflammation in obese mice by inhibiting inflammatory signaling and chemotaxis and decreasing the release of proinflammatory cytokines.[57] Because FFAR4 is expressed in circulating lymphocytes and resident peritoneal macrophages, it is possible that modulated immune activation of these cells by mediators such as prostaglandin E_2 could indirectly influence the artery wall and surrounding PVAT.

Long-chain ω3 PUFAs such as DHA, EPA, and α-linolenic acid detected in *fat-1* mice have all been reported to activate FFAR4.[37,58–60] In our current study, we were unable to discern which of these was most efficacious or whether the effects presented were the combined contribution of all ω3 PUFAs in the body. Alternative pathways can explain the beneficial actions of ω3 PUFAs, including generation of DHA- and/or EPA-derived specialized proresolving mediators.[61] DHA-derived resolvin D1 or neuroprotectin specialized proresolving mediators confer anti-inflammatory and proresolving actions in inflamed tissues.[62,63] Resolvin D2 given to mice within 4 hours after burn effectively prevented thrombosis of the deep dermal vascular network.[64] Resolvin E1 in human whole blood inhibits leukocyte activation and rolling by regulating rapid L-selectin shedding and selectively blocks ADP-stimulated platelet aggregation.[65] Although specialized proresolving mediators may mediate some of the salutary actions of ω3 PUFAs, they do not appear to act via FFAR4.

In summary, the in vivo data presented combined with our previous in vitro data[15] support a mechanism by which activation of the ω3 PUFA–FFAR4 axis results in fewer detrimental effects on postinjury blood flow, reduced neointimal hyperplasia, and limited macrophage migration. A growing number of studies support the unique role of FFAR4 in modulating inflammation and mitigating obesity. It will be interesting to investigate the role of FFAR4 activation in the pathological process of arterial thrombosis and atherosclerosis in the context of obesity, insulin resistance, and other metabolic disorders. Our investigations pave the way for better understanding of the ω3 PUFA–FFAR4 pathway and crosstalk of perivascular and vascular cells in cardiovascular disorders. In the long term, this research should shed light on cardiovascular inflammatory cascades and will provide novel therapeutic evidence for ω3 PUFAs and possibly FFAR4 agonists for the management of vascular events.

Acknowledgments

We thank Mr. J. Durelle and Dr. P. Jessop Department of Chemistry, Queen's University for expert technical assistance in gas

chromatography analysis. We also acknowledge Dr Bingshu Chen (NCIC Clinical Trials Group and Department of Community Health and Epidemiology, Queen's University) for data analysis.

Sources of Funding

This work was supported by the Joint Health Research Initiative between the Canadian Institutes for Health Research and the National Natural Science Foundation of China (CCI 117951 and NSFC 81161120538). Dr. Funk holds a Tier I Canada Research Chair in Molecular, Cellular and Physiological Medicine and is recipient of a Career Investigator Award from the Heart and Stroke Foundation of Ontario.

Disclosures

None.

References

1. Bang HO, Dyerberg J, Nielsen AB. Plasma lipid and lipoprotein pattern in greenlandic West-coast Eskimos. *Lancet*. 1971;1:1143–1145.
2. Dyerberg J, Bang HO, Stoffersen E, Moncada S, Vane JR. Eicosapentaenoic acid and prevention of thrombosis and atherosclerosis? *Lancet*. 1978;2:117–119.
3. Yokoyama M, Origasa H, Matsuzaki M, Matsuzawa Y, Saito Y, Ishikawa Y, Oikawa S, Sasaki J, Hishida H, Itakura H, Kita T, Kitabatake A, Nakaya N, Sakata T, Shimada K, Shirato K; Japan EPAlisl. Effects of eicosapentaenoic acid on major coronary events in hypercholesterolaemic patients (JELIS): a randomised open-label, blinded endpoint analysis. *Lancet*. 2007;369:1090–1098.
4. Marszalek JR, Lodish HF. Docosahexaenoic acid, fatty acid-interacting proteins, and neuronal function: breastmilk and fish are good for you. *Annu Rev Cell Dev Biol*. 2005;21:633–657.
5. Calviello G, Di Nicuolo F, Gragnoli S, Piccioni E, Serini S, Maggiano N, Tringali G, Navarra P, Ranelletti FO, Palozza P. N-3 PUFAs reduce VEGF expression in human colon cancer cells modulating the COX-2/PGE2 induced ERK-1 and -2 and HIF-1alpha induction pathway. *Carcinogenesis*. 2004;25:2303–2310.
6. De Caterina R. N-3 fatty acids in cardiovascular disease. *N Engl J Med*. 2011;364:2439–2450.
7. Smith WL. Cyclooxygenases, peroxide tone and the allure of fish oil. *Curr Opin Cell Biol*. 2005;17:174–182.
8. Faggin E, Puato M, Chiavegato A, Franch R, Pauletto P, Sartore S. Fish oil supplementation prevents neointima formation in nonhypercholesterolemic balloon-injured rabbit carotid artery by reducing medial and adventitial cell activation. *Arterioscler Thromb Vasc Biol*. 2000;20:152–163.
9. Pakala R, Pakala R, Benedict C. Eicosapentaenoic acid and docosahexaenoic acid selectively attenuate U46619-induced smooth muscle cell proliferation. *Lipids*. 1999;34:915–920.
10. Kromhout D, Giltay EJ, Geleijnse JM. N-3 fatty acids and cardiovascular events after myocardial infarction. *N Engl J Med*. 2010;363:2015–2026.
11. Bosch J, Gerstein HC, Dagenais GR, Diaz R, Dyal L, Jung H, Maggiono AP, Probstfield J, Ramachandran A, Riddle MC, Ryden LE, Yusuf S. N-3 fatty acids and cardiovascular outcomes in patients with dysglycemia. *N Engl J Med*. 2012;367:309–318.
12. Roncaglioni MC, Tombesi M, Avanzini F, Barlera S, Caimi V, Longoni P, Marzona I, Milani V, Silletta MG, Tognoni G, Marchioli R. N-3 fatty acids in patients with multiple cardiovascular risk factors. *N Engl J Med*. 2013;368:1800–1808.
13. Oh DY, Talukdar S, Bae EJ, Imamura T, Morinaga H, Fan W, Li P, Lu WJ, Watkins SM, Olefsky JM. GPR120 is an omega-3 fatty acid receptor mediating potent anti-inflammatory and insulin-sensitizing effects. *Cell*. 2010;142:687–698.
14. Ichimura A, Hirasawa A, Poulain-Godefroy O, Bonnefond A, Hara T, Yengo L, Kimura I, Leloire A, Liu N, Iida K, Choquet H, Besnard P, Lecoeur C, Vivequin S, Ayukawa K, Takeuchi M, Ozawa K, Tauber M, Maffeis C, Morandi A, Buzzetti R, Elliott P, Pouta A, Jarvelin MR, Korner A, Kiess W, Pigeyre M, Caiazzo R, Van Hul W, Van Gaal L, Horber F, Balkau B, Levy-Marchal C, Rouskas K, Kouvatsi A, Hebebrand J, Hinney A, Scherag A, Pattou F, Meyre D, Koshimizu TA, Wolowczuk I, Tsujimoto G, Froguel P. Dysfunction of lipid sensor GPR120 leads to obesity in both mouse and human. *Nature*. 2012;483:350–354.
15. Li X, Yu Y, Funk CD. Cyclooxygenase-2 induction in macrophages is modulated by docosahexaenoic acid via interactions with free fatty acid receptor 4 (FFA4). *FASEB J*. 2013;27:4987–4997.
16. Liu Y, Chen LY, Sokolowska M, Eberlein M, Alsaaty S, Martinez-Anton A, Logun C, Qi HY, Shelhamer JH. The fish oil ingredient, docosahexaenoic acid, activates cytosolic phospholipase A via GPR120 receptor to produce prostaglandin E and plays an anti-inflammatory role in macrophages. *Immunology*. 2014;143:81–95.
17. Wellhauser L, Belsham DD. Activation of the omega-3 fatty acid receptor GPR120 mediates anti-inflammatory actions in immortalized hypothalamic neurons. *J Neuroinflammation*. 2014;11:60.
18. Williams-Bey Y, Boularan C, Vural A, Huang NN, Hwang IY, Shan-Shi C, Kehrl JH. Omega-3 free fatty acids suppress macrophage inflammasome activation by inhibiting NF-kappaB activation and enhancing autophagy. *PLoS One*. 2014;9:e97957.
19. von Hundelshausen P, Weber C. Platelets as immune cells: bridging inflammation and cardiovascular disease. *Circ Res*. 2007;100:27–40.
20. Libby P, Ridker PM, Hansson GK. Inflammation in atherosclerosis: from pathophysiology to practice. *J Am Coll Cardiol*. 2009;54:2129–2138.
21. Chatterjee TK, Stoll LL, Denning GM, Harrelson A, Blomkalns AL, Idelman G, Rothenberg FG, Neltner B, Romig-Martin SA, Dickson EW, Rudich S, Weintraub NL. Proinflammatory phenotype of perivascular adipocytes: influence of high-fat feeding. *Circ Res*. 2009;104:541–549.
22. Kang JX, Wang J, Wu L, Kang ZB. Transgenic mice: fat-1 mice convert n-6 to n-3 fatty acids. *Nature*. 2004;427:504.
23. Valenzuela DM, Murphy AJ, Frendewey D, Gale NW, Economides AN, Auerbach W, Poueymirou WT, Adams NC, Rojas J, Yasenchak J, Chernomorsky R, Boucher M, Elsasser AL, Esau L, Zheng J, Griffiths JA, Wang X, Su H, Xue Y, Dominguez MG, Noguera I, Torres R, Macdonald LE, Stewart AF, DeChiara TM, Yancopoulos GD. High-throughput engineering of the mouse genome coupled with high-resolution expression analysis. *Nat Biotechnol*. 2003;21:652–659.
24. Boudrault C, Bazinet RP, Kang JX, Ma DW. Cyclooxygenase-2 and n-6 PUFA are lower and DHA is higher in the cortex of fat-1 mice. *Neurochem Int*. 2010;56:585–589.
25. Kang JX, Wang J. A simplified method for analysis of polyunsaturated fatty acids. *BMC Biochem*. 2005;6:5.
26. Poeckel D, Zemski Berry KA, Murphy RC, Funk CD. Dual 12/15- and 5-lipoxygenase deficiency in macrophages alters arachidonic acid metabolism and attenuates peritonitis and atherosclerosis in ApoE knock-out mice. *J Biol Chem*. 2009;284:21077–21089.
27. Barajas-Espinosa A, Ni NC, Yan D, Zarini S, Murphy RC, Funk CD. The cysteinyl leukotriene 2 receptor mediates retinal edema and pathological neovascularization in a murine model of oxygen-induced retinopathy. *FASEB J*. 2012;26:1100–1109.
28. Bonheur JA, Albadawi H, Patton GM, Watkins MT. A noninvasive murine model of hind limb ischemia-reperfusion injury. *J Surg Res*. 2004;116:55–63.
29. Ouma GO, Rodriguez E, Muthumani K, Weiner DB, Wilensky RL, Mohler ER III. In vivo electroporation of constitutively expressed HIF-1alpha plasmid DNA improves neovascularization in a mouse model of limb ischemia. *J Vasc Surg*. 2014;59:786–793.
30. Evans DJ, Jackman LE, Chamberlain J, Crosdale DJ, Judge HM, Jetha K, Norman KE, Francis SE, Storey RF. Platelet P2Y(12) receptor influences the vessel wall response to arterial injury and thrombosis. *Circulation*. 2009;119:116–122.
31. Kawasaki T, Taniguchi M, Moritani Y, Uemura T, Shigenaga T, Takamatsu H, Hayashi K, Takasaki J, Saito T, Nagai K. Pharmacological properties of YM-254890, a specific G(alpha)q/11 inhibitor, on thrombosis and neointima formation in mice. *Thromb Haemost*. 2005;94:184–192.
32. Cao RY, Adams MA, Habenicht AJ, Funk CD. Angiotensin II-induced abdominal aortic aneurysm occurs independently of the 5-lipoxygenase pathway in apolipoprotein E-deficient mice. *Prostaglandins Other Lipid Mediat*. 2007;84:34–42.
33. Cao RY, St Amand T, Li X, Yoon SH, Wang CP, Song H, Maruyama T, Brown PM, Zelt DT, Funk CD. Prostaglandin receptor EP4 in abdominal aortic aneurysms. *Am J Pathol*. 2012;181:313–321.
34. Yu Y, Ricciotti E, Scalia R, Tang SY, Grant G, Yu Z, Landesberg G, Crichton I, Wu W, Pure E, Funk CD, FitzGerald GA. Vascular COX-2 modulates blood pressure and thrombosis in mice. *Sci Transl Med*. 2012;4:132ra154.
35. Fehrenbach ML, Cao G, Williams JT, Finklestein JM, Delisser HM. Isolation of murine lung endothelial cells. *Am J Physiol Lung Cell Mol Physiol*. 2009;296:L1096–L1103.
36. Ni NC, Yan D, Ballantyne LL, Barajas-Espinosa A, St Amand T, Pratt DA, Funk CD. A selective cysteinyl leukotriene receptor 2 antagonist blocks myocardial

ischemia/reperfusion injury and vascular permeability in mice. *J Pharmacol Exp Ther*. 2011;339:768–778.

37. Hirasawa A, Tsumaya K, Awaji T, Katsuma S, Adachi T, Yamada M, Sugimoto Y, Miyazaki S, Tsujimoto G. Free fatty acids regulate gut incretin glucagon-like peptide-1 secretion through GPR120. *Nat Med*. 2005;11:90–94.
38. Watts JL, Browse J. Genetic dissection of polyunsaturated fatty acid synthesis in *Caenorhabditis elegans*. *Proc Natl Acad Sci USA*. 2002;99:5854–5859.
39. Romanatto T, Fiamoncini J, Wang B, Curi R, Kang JX. Elevated tissue omega-3 fatty acid status prevents age-related glucose intolerance in fat-1 transgenic mice. *Biochim Biophys Acta*. 2014;1842:186–191.
40. Eckly A, Hechler B, Freund M, Zerr M, Cazenave JP, Lanza F, Mangin PH, Gachet C. Mechanisms underlying $FeCl_3$-induced arterial thrombosis. *J Thromb Haemost*. 2011;9:779–789.
41. Takaoka M, Nagata D, Kihara S, Shimomura I, Kimura Y, Tabata Y, Saito Y, Nagai R, Sata M. Periadventitial adipose tissue plays a critical role in vascular remodeling. *Circ Res*. 2009;105:906–911.
42. Omar A, Chatterjee TK, Tang Y, Hui DY, Weintraub NL. Proinflammatory phenotype of perivascular adipocytes. *Arterioscler Thromb Vasc Biol*. 2014;34:1631–1636.
43. Rizos EC, Ntzani EE, Bika E, Kostapanos MS, Elisaf MS. Association between omega-3 fatty acid supplementation and risk of major cardiovascular disease events: a systematic review and meta-analysis. *JAMA*. 2012;308:1024–1033.
44. Withers SB, Bussey CE, Saxton SN, Melrose HM, Watkins AE, Heagerty AM. Mechanisms of adiponectin-associated perivascular function in vascular disease. *Arterioscler Thromb Vasc Biol*. 2014;34:1637–1642.
45. Brown NK, Zhou Z, Zhang J, Zeng R, Wu J, Eitzman DT, Chen YE, Chang L. Perivascular adipose tissue in vascular function and disease: a review of current research and animal models. *Arterioscler Thromb Vasc Biol*. 2014;34:1621–1630.
46. Britton KA, Fox CS. Perivascular adipose tissue and vascular disease. *Clin Lipidol*. 2011;6:79–91.
47. Minotti G, Aust SD. The requirement for iron (III) in the initiation of lipid peroxidation by iron (II) and hydrogen peroxide. *J Biol Chem*. 1987;262:1098–1104.
48. Chang L, Villacorta L, Li R, Hamblin M, Xu W, Dou C, Zhang J, Wu J, Zeng R, Chen YE. Loss of perivascular adipose tissue on peroxisome proliferator-activated receptor-gamma deletion in smooth muscle cells impairs intravascular thermoregulation and enhances atherosclerosis. *Circulation*. 2012;126:1067–1078.
49. Manka D, Chatterjee TK, Stoll LL, Basford JE, Konaniah ES, Srinivasan R, Bogdanov VY, Tang Y, Blomkalns AL, Hui DY, Weintraub NL. Transplanted perivascular adipose tissue accelerates injury-induced neointimal hyperplasia: role of monocyte chemoattractant protein-1. *Arterioscler Thromb Vasc Biol*. 2014;34:1723–1730.
50. Sata M, Maejima Y, Adachi F, Fukino K, Saiura A, Sugiura S, Aoyagi T, Imai Y, Kurihara H, Kimura K, Omata M, Makuuchi M, Hirata Y, Nagai R. A mouse model of vascular injury that induces rapid onset of medial cell apoptosis followed by reproducible neointimal hyperplasia. *J Mol Cell Cardiol*. 2000;32:2097–2104.
51. Ruzickova J, Rossmeisl M, Prazak T, Flachs P, Sponarova J, Veck M, Tvrzicka E, Bryhn M, Kopecky J. Omega-3 PUFA of marine origin limit diet-induced obesity in mice by reducing cellularity of adipose tissue. *Lipids*. 2004;39:1177–1185.
52. Kim W, Barhoumi R, McMurray DN, Chapkin RS. Dietary fish oil and DHA down-regulate antigen-activated CD4+ T-cells while promoting the formation of liquid-ordered mesodomains. *Br J Nutr*. 2014;111:254–260.
53. Gong Y, Lin M, Piao L, Li X, Yang F, Zhang J, Xiao B, Zhang Q, Song WL, Yin H, Zhu L, Funk CD, Yu Y. Aspirin enhances protective effect of fish oil against thrombosis and injury-induced vascular remodeling. *Br J Pharmacol*. 2015; doi: 10.1111/bph.12986 [Epub ahead of print].
54. Dyerberg J, Bang HO. Haemostatic function and platelet polyunsaturated fatty acids in Eskimos. *Lancet*. 1979;2:433–435.
55. Goodnight SH Jr, Harris WS, Connor WE. The effects of dietary omega 3 fatty acids on platelet composition and function in man: a prospective, controlled study. *Blood*. 1981;58:880–885.
56. Sukumar P, Sedo A, Li J, Wilson LA, O'Regan D, Lippiat JD, Porter KE, Kearney MT, Ainscough JF, Beech DJ. Constitutively active TRPC channels of adipocytes confer a mechanism for sensing dietary fatty acids and regulating adiponectin. *Circ Res*. 2012;111:191–200.
57. Oh DY, Walenta E, Akiyama TE, Lagakos WS, Lackey D, Pessentheiner AR, Sasik R, Hah N, Chi TJ, Cox JM, Powels MA, Di Salvo J, Sinz C, Watkins SM, Armando AM, Chung H, Evans RM, Quehenberger O, McNelis J, Bogner-Strauss JG, Olefsky JM. A GPR120-selective agonist improves insulin resistance and chronic inflammation in obese mice. *Nat Med*. 2014;20:942–947.
58. Briscoe CP, Peat AJ, McKeown SC, Corbett DF, Goetz AS, Littleton TR, McCoy DC, Kenakin TP, Andrews JL, Ammala C, Fornwald JA, Ignar DM, Jenkinson S. Pharmacological regulation of insulin secretion in MIN6 cells through the fatty acid receptor GPR40: identification of agonist and antagonist small molecules. *Br J Pharmacol*. 2006;148:619–628.
59. Hudson BD, Shimpukade B, Mackenzie AE, Butcher AJ, Pediani JD, Christiansen E, Heathcote H, Tobin AB, Ulven T, Milligan G. The pharmacology of TUG-891, a potent and selective agonist of the free fatty acid receptor 4 (FFA4/GPR120), demonstrates both potential opportunity and possible challenges to therapeutic agonism. *Mol Pharmacol*. 2013;84:710–725.
60. Sparks SM, Chen G, Collins JL, Danger D, Dock ST, Jayawickreme C, Jenkinson S, Laudeman C, Leesnitzer MA, Liang X, Maloney P, McCoy DC, Moncol D, Rash V, Rimele T, Vulimiri P, Way JM, Ross S. Identification of diarylsulfonamides as agonists of the free fatty acid receptor 4 (FFA4/GPR120). *Bioorg Med Chem Lett*. 2014;24:3100–3103.
61. Serhan CN. Pro-resolving lipid mediators are leads for resolution physiology. *Nature*. 2014;510:92–101.
62. Schwab JM, Chiang N, Arita M, Serhan CN. Resolvin E1 and protectin D1 activate inflammation-resolution programmes. *Nature*. 2007;447:869–874.
63. Spite M, Summers L, Porter TF, Srivastava S, Bhatnagar A, Serhan CN. Resolvin D1 controls inflammation initiated by glutathione-lipid conjugates formed during oxidative stress. *Br J Pharmacol*. 2009;158:1062–1073.
64. Bohr S, Patel SJ, Sarin D, Irimia D, Yarmush ML, Berthiaume F. Resolvin D2 prevents secondary thrombosis and necrosis in a mouse burn wound model. *Wound Repair Regen*. 2013;21:35–43.
65. Dona M, Fredman G, Schwab JM, Chiang N, Arita M, Goodarzi A, Cheng G, von Andrian UH, Serhan CN. Resolvin E1, an EPA-derived mediator in whole blood, selectively counterregulates leukocytes and platelets. *Blood*. 2008;112:848–855.